Research article

NMR IN BIOMEDICINE

Received: 28 May 2013, Revised: 8 October 2013, Accepted: 10 October 2013, Published online in Wiley Online Library: 24 November 2013

(wileyonlinelibrary.com) DOI: 10.1002/nbm.3050

Reliability of MRSI brain temperature mapping at 1.5 and 3 T

Michael J. Thrippleton[a], Jehill Parikh[a], Bridget A. Harris[b], Steven J. Hammer[c], Scott I. K. Semple[d], Peter J. D. Andrews[e], Joanna M. Wardlaw[a] and Ian Marshall[a]*

MRSI permits the non-invasive mapping of brain temperature *in vivo*, but information regarding its reliability is lacking. We obtained MRSI data from 31 healthy male volunteers [age range, 22–40 years; mean ± standard deviation (SD), 30.5 ± 5.0 years]. Eleven subjects (age range, 23–40 years; mean ± SD, 30.5 ± 5.2 years) were invited to receive four point-resolved spectroscopy MRSI scans on each of 3 days in both 1.5-T (TR/TE = 1000/144 ms) and 3-T (TR/TE = 1700/144 ms) clinical scanners; a further 20 subjects (age range, 22–40 years; mean ± SD, 30.5 ± 4.9 years) were scanned on a single occasion at 3 T. Data were fitted in the time domain to determine the water–*N*-acetylaspartate chemical shift difference, from which the temperature was estimated. Temperature data were analysed using a linear mixed effects model to determine variance components and systematic temperature changes during the scanning sessions. To characterise the effects of instrumental drift on apparent MRSI brain temperature, a temperature-controlled phantom was constructed and scanned on multiple occasions. Components of apparent *in vivo* temperature variability at 1.5 T/3 T caused by inter-subject (0.18/0.17 °C), inter-session (0.18/0.15 °C) and within-session (0.36/0.14 °C) effects, as well as voxel-to-voxel variation (0.59/0.54 °C), were determined. There was a brain cooling effect during *in vivo* MRSI of 0.10 °C [95% confidence interval (CI): −0.110, −0.094 °C; $p < 0.001$] and 0.051 °C (95% CI: −0.054, −0.048 °C; $p < 0.001$) per scan at 1.5 T and 3 T, respectively, whereas phantom measurements revealed minimal drift in apparent MRSI temperature relative to fibre-optic temperature measurements. The mean brain temperature at 3 T was weakly associated with aural ($R = 0.55$, $p = 0.002$) and oral ($R = 0.62$, $p < 0.001$) measurements of head temperature. In conclusion, the variability associated with MRSI brain temperature mapping was quantified. Repeatability was somewhat higher at 3 T than at 1.5 T, although subtle spatial and temporal variations in apparent temperature were demonstrated at both field strengths. Such data should assist in the efficient design of future clinical studies. © 2013 The Authors. *NMR in Biomedicine* published by John Wiley & Sons, Ltd.

Keywords: spectroscopic imaging; spectroscopic quantification; normal brain; temperature; thermometry

INTRODUCTION

Temperature is an important physiological parameter in illness, particularly after stroke and traumatic brain injury, in which pyrexia is common and associated with a worse outcome (1). Temperature management is therefore part of standard care in brain-injured patients, and a temperature decrease of as little as 0.3 °C may be clinically relevant (2,3). Although whole-body cooling interventions have most commonly been used, the likely importance of temperature at the site of injury (i.e. the brain) has led to interest in the development of improved head cooling methods (4). Unfortunately, conventional methods for the measurement of brain temperature are invasive, unsuitable for all but the most severely ill, and restrict the number and location of sampling sites. Consequently, the effects on brain temperature of temperature interventions and the nature of its relationship to body temperature and outcome following different brain injuries remain poorly understood (5), and there has therefore been considerable interest in non-invasive MRI-based temperature measurement.

* *Correspondence to: I. Marshall, Professor of Magnetic Resonance Physics, School of Clinical Sciences, University of Edinburgh, Medical Physics, Western General Hospital, Edinburgh EH4 2XU, UK.*
E-mail: ian.marshall@ed.ac.uk

a *M. J. Thrippleton, J. Parikh, J. M. Wardlaw, I. Marshall*
Brain Research Imaging Centre, Centre for Clinical Brain Sciences, University of Edinburgh, Edinburgh, UK

b *B. A. Harris*
Critical Care, NHS Lothian, Edinburgh, UK

c *S. J. Hammer*
School of Engineering and Physical Sciences, Heriot-Watt University, Edinburgh, UK

d *S. I. K. Semple*
Clinical Research Imaging Centre, Centre for Cardiovascular Sciences, University of Edinburgh, Edinburgh, UK

e *P. J. D. Andrews*
Centre for Clinical Brain Sciences, University of Edinburgh, Edinburgh, UK

Abbreviations used: *CI, confidence interval; CSF, cerebrospinal fluid; FID, free induction decay; GE, gradient echo; GM, grey matter; NAA, N-acetylaspartate; PRESS, point-resolved spectroscopy; SD, standard deviation; T2W, T_2-weighted; WM, white matter.*

Although a number of measurable MR quantities are temperature dependent (6), the most widely exploited of these is the water chemical shift, which has a temperature dependence of −0.01 ppm/°C. This property is used in phase shift techniques, permitting relatively high-resolution mapping of short-timescale temperature changes, although not of absolute temperatures (7). However, these methods are susceptible to temporal and spatial variation in the scanner magnetic field, and have therefore mainly been used to measure large within-scan temperature changes, such as those which occur during thermal ablation therapy. More subtle temporal or spatial variations in brain temperature have been assessed using MRS techniques (8,9), in which the measurement of a chemical shift difference [e.g. that between water and *N*-acetylaspartate (NAA)] permits the estimation of the 'absolute' temperature with fewer confounding effects (10). Data are often acquired from a single voxel of interest; however, two- or three-dimensional temperature maps may be obtained using MRSI (11,12), which has recently been applied in acute ischaemic stroke to explore group-level regional variation and time dependence of brain temperature following stroke (13,14), and the relationship with acute inflammation response markers (15).

However, despite recent applications in healthy volunteers and patients, little information regarding the reliability of MRSI temperature measurements is available to assist in the planning and interpretation of clinical studies. Marshall *et al.* (12) performed a validation study at 1.5 T, finding a standard deviation (SD) of 1.2 °C for repeated measurements on individual voxels; this was a small study (four subjects), however, and repeated measurements were obtained during a single examination. Childs *et al.* (11) scanned eight healthy subjects, comparing differences between temperatures obtained by single-voxel MRS and MRSI techniques, and concluding that there was greater uncertainty in MRSI temperature estimates; however, repeated measurements were not performed.

The aim of this study was to characterise the reliability of MRSI thermometry, including contributions from inter-scan and inter-examination variability. In addition, we sought to measure the variation between subjects and to assess the extent of within-brain temperature variation. With 3-T MR scanners now in common use in the research environment, we further aimed to determine whether the theoretical benefits of a higher magnetic field strength result in more reliable temperature mapping, and therefore obtained data at both 1.5 and 3 T. To determine whether potential scanner instability results in drifts in apparent brain temperature, we performed additional experiments using a temperature-controlled phantom.

EXPERIMENTAL DETAILS

Study design

Following approval by the Local Research Ethics Committee, we recruited 31 healthy volunteers in the age range 22–40 years (mean ± SD, 30.5 ± 5.0 years); to exclude the influence of body temperature variation during the menstrual cycle, only male subjects were recruited. All scans were performed in the afternoon to minimise the influence of diurnal temperature variation, and participants were asked to refrain from eating, drinking, exercising and spending any time outdoors for 1 h prior to scanning; all participants wore surgical scrubs and the temperatures of the scanner rooms were regulated and monitored. Eleven subjects (age range, 23–40 years; mean ± SD, 30.5 ± 5.2 years) were invited for scanning on three occasions in both 1.5 and 3-T scanners; four MRSI temperature scans were obtained consecutively on each occasion. A further 20 subjects (age range, 22–40 years; mean ± SD, 30.5 ± 4.9 years) received a single MRSI scan at 3 T. Oral (WelshAllyn SureTemp 678, WelchAllyn, Aston Abbotts, UK) and tympanic (Genius™ 2, Covidien, Gosport, UK) temperatures were measured before and after scanning, using the same sublingual pocket and ear each time within subjects.

MRI

Scanning at 1.5 T was performed using a GE Signa Horizon HDx clinical scanner (GE Healthcare, Slough, UK) fitted with a transmit–receive quadrature head coil. Temperature data were obtained using a single-slice point-resolved spectroscopy (PRESS) MRSI sequence [TR/TE = 1000/144 ms; field of view, 300 × 300 mm^2) with 24-step phase encoding in both in-plane directions. A single 10-mm slice was located axially at the level of the superior part of the corpus callosum using axial T_2-weighted (T2W) and sagittal localiser images for planning, as shown in Fig. 1a, b. Four saturation bands were applied to suppress scalp lipid signals and the excitation region was restricted to the anterior extent of the corpus callosum to minimise signal from regions with poor magnetic field homogeneity. Automated shimming and chemical shift-selective water suppression, which was adjusted to retain a residual water signal, were applied. For each phase-encoding step, a 512-ms free induction decay (FID) was obtained with a dwell time of 1 ms. The MRSI scanning time was approximately 9 min 40 s in addition to prescan optimisation, which was performed before every acquisition. Localisers and axial T2W scans (two-dimensional fast spin-echo sequence; TR/TE = 11 320/102 ms; matrix, 256 × 256; field of view, 256 × 256 mm^2; contiguous slices 2 mm thick) were acquired prior to MRSI to facilitate the placement of the volume of interest. Additional T_1-weighted (T1W; three-dimensional inversion-recovery-prepared gradient echo (GE); TR/TI/TE = 9.6/500/4.0 ms; flip angle, 8°; isotropic resolution, 1.3 mm) and axial two-dimensional GE (TR/TE = 940/15 ms; flip angle, 20°; matrix, 256 × 192; field of view, 256 × 256 mm^2; contiguous slices 2 mm thick) scans were acquired at the first visit only.

Scanning at 3 T was performed using a Magnetom Verio 3-T clinical scanner (Siemens AG, Healthcare Sector, Erlangen, Germany) equipped with a 12-channel receive-only head coil. MRSI data were obtained as described above using a semi-LASER PRESS MRSI sequence (16) (TR/TE = 1700/144 ms); elliptical *k*-space sampling was used to achieve a similar scan time (approximately 10 min 50 s) to the 1.5-T acquisition; data from the coil elements were phase corrected individually and combined in the time domain using the manufacturer-provided algorithm (17). Localisers and axial T2W (two-dimensional fast spin-echo; TR/TE = 13 241/98 ms; matrix, 256 × 256; field of view, 256 × 256 mm; contiguous slices 2 mm thick) were acquired prior to MRSI, and T1W (three-dimensional inversion-recovery-prepared GE; TR/TI/TE = 2300/900/2.98 ms; flip angle, 9°; isotropic resolution, 1 mm) and axial three-dimensional GE (TR/TE = 27/10 ms; flip angle, 15°; matrix, 256 × 256; field of view, 256 × 256 mm; slice thickness, 2 mm) scans were obtained at the first visit.

Data analysis

MRSI data, interpolated to 32 × 32 voxels (nominal dimensions, 9.375 × 9.375 × 10 mm^3) by zero filling of the *k*-space data, were corrected for phase and eddy current distortion using the residual

NMR IN BIOMEDICINE

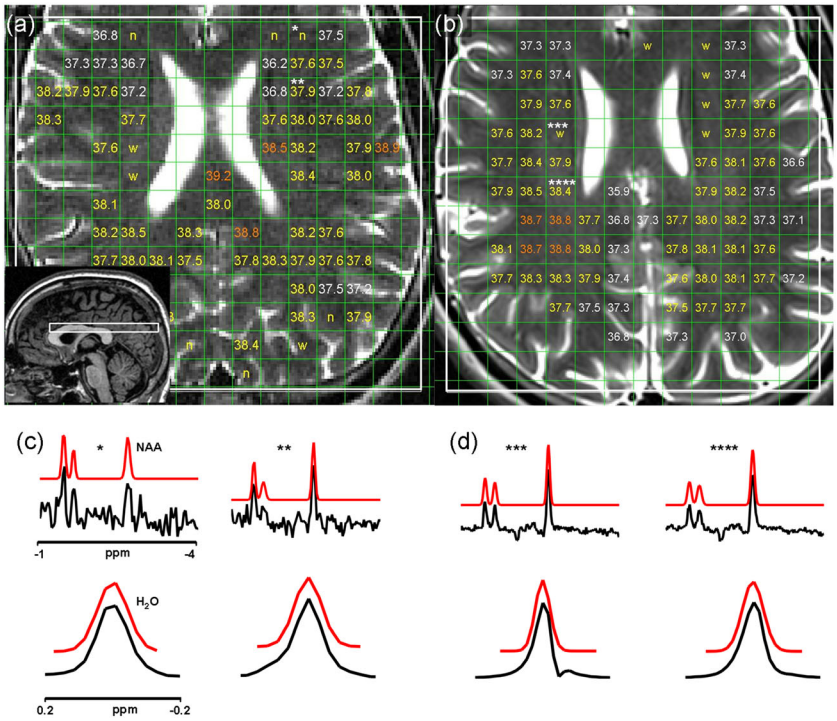

Figure 1. The 1.5-T (a) and 3-T (b) T_2-weighted (T2W) images of one subject overlaid with MRSI excitation volumes (white) and temperature estimates. 'n' indicates voxels rejected as a result of poor quality of *N*-acetylaspartate (NAA) fitting, and 'w' indicates voxels rejected as a result of distortions of the water resonance. Voxels covering >5% cerebrospinal fluid (CSF) or non-brain regions are empty (note that some voxels are rejected because of CSF that is not visible in the 2-mm-thick T2W image displayed). The sagittal localiser image used to position the volume of interest is shown as the inset in (a). (c) and (d) show acquired (black) and simulated (based on fitted parameters; red) spectra corresponding to representative voxels labelled in (a) and (b), respectively. The voxel labelled '*' was rejected because of poor NAA fit quality, as the resonance is close to the noise level; the voxel labelled '***' was rejected because of a distorted asymmetric water resonance; the remaining two voxels were accepted. Chemical shifts are displayed relative to the water resonance.

water signal, shifting the water resonance to zero frequency (18); the frequency difference between water and NAA ($\Delta\delta$, ppm) was determined by time-domain fitting of the NAA resonance with a Gaussian lineshape model using the AMARES algorithm (19), following removal of the water resonance [HLSVD algorithm (20)] with the JMRUI software package (21). The success of the fitting procedure was determined automatically by calculating the coefficient of determination for the model in the region ±0.1 ppm of the NAA resonance; the threshold for acceptance ($R^2 \geq 0.8$) was determined visually in order to exclude voxels in which a NAA resonance was not clearly visible above the noise or in which the NAA resonance had been 'missed' by the fitting algorithm. Fits yielding zero NAA amplitude were also rejected. To exclude spectra that had distorted water lineshapes, the water resonance was fitted using a frequency-domain Gaussian model in the region ±0.15 ppm of the resonance and the coefficient of determination was used to determine acceptance (threshold $R^2 \geq 0.965$); this was performed prior to the eddy current correction described above and was used only to assess spectral quality (the water frequency is set to zero by the eddy current correction, so that further fitting is not required to determine the temperature). Temperature was calculated as described previously (12) using the relationship T (°C) = 37 − 100($\Delta\delta$ − 2.665).

T1W and GE images obtained at the first visit were co-registered to T2W scans using FSL FLIRT (22); brain masks were derived from GE images using FSL BET2 (23), and were applied to T1W images, from which tissue segmentation images were generated using FSL FAST (24). Voxels covering regions containing >5% cerebrospinal fluid (CSF) or >5% non-brain were excluded from the analysis. For each visit, a line dividing the left and right cerebral hemispheres was drawn manually on T2W images and used to classify voxels by hemisphere.

Statistics

Temperature data were analysed using the mixed linear effects model procedure in PASW version 18 (IBM Corporation, Armonk, NY, USA). Correlations were assessed using Pearson's correlation coefficient in Matlab (Mathworks, Natick, MA, USA), as were *t*-tests for paired and unpaired differences. $p < 0.05$ (two-sided) was considered to be significant in statistical tests.

Phantom experiments

A spherical acrylic phantom (diameter, 18 cm) divided into two hemispheres, each containing a smaller sphere (diameter, 6 cm), was constructed (Fig. 2a). The two inner spheres were filled with an aqueous solution containing metabolites at approximate physiological concentrations [10.3 mM NAA, 1.7 mM *N*-acetylaspartylglutamate, 10 mM creatine hydrate, 3 mM choline chloride, 7.5 mM myo-inositol, 12.5 mM glutamate, 5 mM lactate, 0.1% w/v sodium azide and 0.1% v/v gadoteric acid (0.5 M; DOTAREM, Guerbet, France), buffered with 50 mM monobasic potassium phosphate and 56 mM sodium hydroxide]. Heated water baths were used to circulate water around the outside of the metabolite compartments, maintaining the temperature

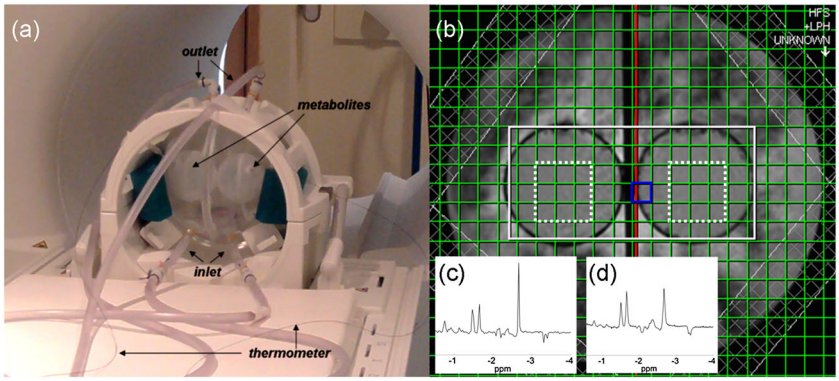

Figure 2. (a) Temperature-controlled phantom positioned in the 3-T scanner, showing points of entry and exit of temperature-controlled water, inner metabolite-containing spheres and fibre-optic thermometer probes leading to the metabolite spheres. (b) The 3-T axial localiser image showing the MRSI excitation volume (white) and central voxels included in the analysis (dotted white line). Typical 1.5-T (c) and 3-T (d) spectra are shown as insets; chemical shifts are displayed relative to the water resonance.

of the left and right hemispheres at 37.0 and 37.5 °C, respectively. The true metabolite temperatures were monitored using MR-compatible fluoroptic thermometer probes (Luxtron 812, LumaSense Technologies Inc., Santa Clara, CA, USA; 0.1 °C accuracy). Five MRSI temperature scans were obtained back-to-back on four occasions at both 1.5 and 3 T. Phantom data were acquired and processed as described above, with the volume of interest covering the two inner spheres (Fig. 2b); the central 3×3 voxels in each inner sphere were analysed. Drifts in apparent MR temperature relative to the gold standard fibre-optic temperature measurements were estimated using a linear mixed effects model.

RESULTS

We obtained valid temperature data from all of the scanning visits. One subject withdrew following the first 1.5-T scanning visit; a second subject attended three 3-T visits, but only one 1.5-T visit; a single 1.5-T MRSI scan was excluded from the analysis because of failure of the scanner optimisation procedure. In total, 11 and 30 subjects were scanned at least once at 1.5 and 3 T, respectively. Among 'brain voxels' [covering at least 95% grey matter (GM)/white matter (WM)/CSF), 52% and 51% of voxels covering >5% CSF were removed from the analysis at 1.5 and 3 T, respectively (mean over all scans); 10.4% and 2.1% (mean) of the retained voxels were disregarded because of poor fitting of the NAA resonance, followed by the rejection of a further 6.2% and 12.4% because of distortions of the water resonance; in total, 40% and 42% of available brain voxels were analysed. Example brain temperature maps and MRSI spectra are shown in Fig. 1. The average temperatures of all accepted voxels (mean ± SD) were 37.7 ± 0.7 and 37.4 ± 0.6 °C at 1.5 and 3 T, respectively; corresponding NAA linewidths were 4.7 ± 1.0 and 8.1 ± 1.8 Hz. The mean room temperatures were 21.2 ± 0.4 and 21.1 ± 0.9 °C at 1.5 and 3 T, respectively.

Inter-subject, inter-day, inter-scan and inter-voxel variation

The 1.5-T (11 subjects) and 3-T (30 subjects) MRSI data were analysed separately using a linear mixed effects model (Table 1), including the random effects of subject, visit and voxel number; the scan number within a session was included in the model as a continuous factor to account for systematic heating or cooling during the session. Inter-subject, inter-visit and inter-voxel variations were similar for the two scanners. The error associated with repeat scanning within a session (i.e. the residual variance) was 0.36 °C at 1.5 T and 0.14 °C at 3 T. The largest single variance component at either field strength was that caused by the variation between voxels. The data also showed a significant ($p < 0.001$) brain cooling effect during back-to-back MRSI scanning, equivalent to 0.10 and 0.05 °C per MRSI scan (scan duration of approximately 12–14 min including scanner optimisation) at 1.5 and 3 T, respectively. Among the 11 subjects that attended sessions with multiple MRSI scans, the mean temperatures of all accepted voxels at 1.5 T were 37.9 ± 0.7, 37.7 ± 0.7, 37.6 ± 0.7 and 37.6 ± 0.7 °C at scans 1–4, respectively; the corresponding temperatures at 3 T were 37.5 ± 0.6, 37.4 ± 0.6, 37.3 ± 0.6 and 37.3 ± 0.6 °C.

Relationship between brain and body temperature

Aural temperature measurements taken before and after the scanning session (averaged over all visits) indicated a significant increase at both 1.5 T (mean over subjects, 0.20 °C; $p = 0.014$) and 3 T (0.38 °C; $p < 0.001$); there was a small mean increase in oral temperature at 3 T (0.10 °C; $p = 0.003$), but not at 1.5 T. MR temperature (averaged in three stages over accepted voxels, scans performed and visits attended) was compared with the corresponding means of pre- and post-scan oral and aural temperature readings (Fig. 3): at 3 T, there was a weak positive correlation between brain temperature and oral temperature ($R = 0.62$, $p < 0.001$) and between brain temperature and aural temperature ($R = 0.55$, $p = 0.002$); a significant association was found only with aural temperature ($R = 0.65$, $p = 0.031$) for the smaller subgroup of subjects scanned at 1.5 T.

Effect of hemisphere and tissue

As within-brain temperature variation was the largest source of variability, further analysis was performed using data from the first MRSI scan for each subject. WM is the most abundant tissue at the slice location chosen, but very few of the MRSI voxels contained a single tissue type; voxels were divided into two categories: those covering regions with ≤25% GM and those covering regions with >25% GM. As shown in Fig. 4, mean left hemisphere voxel temperatures were significantly cooler, on average, than mean right hemisphere voxel temperatures (0.20/0.12 °C temperature difference at 1.5 T/3 T; $p = 0.014/0.002$), and predominantly WM voxels

NMR IN BIOMEDICINE

Table 1. Intercept, variance components and rate of temperature change (β_{scan}) from linear mixed effects model analysis of MRSI temperature data; scans within a session were labelled 0, 1, 2 and 3, so that the intercept is the mean temperature predicted by the model during the first MRSI scan. 95% confidence intervals for parameter estimates are shown in parentheses

	Intercept (°C)	$\sigma_{subject}$ (°C)	σ_{visit} (°C)	σ_{voxel} (°C)	$\sigma_{residual}$ (°C)	β_{scan} (°C/scan)
1.5 T	37.83 (37.67–37.98)	0.18 (0.09–0.36)	0.18 (0.12–0.27)	0.59 (0.57–0.61)	0.363 (0.355–0.370)	−0.102[a] (−0.110 to −0.094)
3 T	37.51 (37.42–37.59)	0.17 (0.09–0.32)	0.15 (0.09–0.24)	0.54 (0.53–0.56)	0.145 (0.142–0.148)	−0.051[a] (−0.054 to −0.048)

[a] $p < 0.001$.

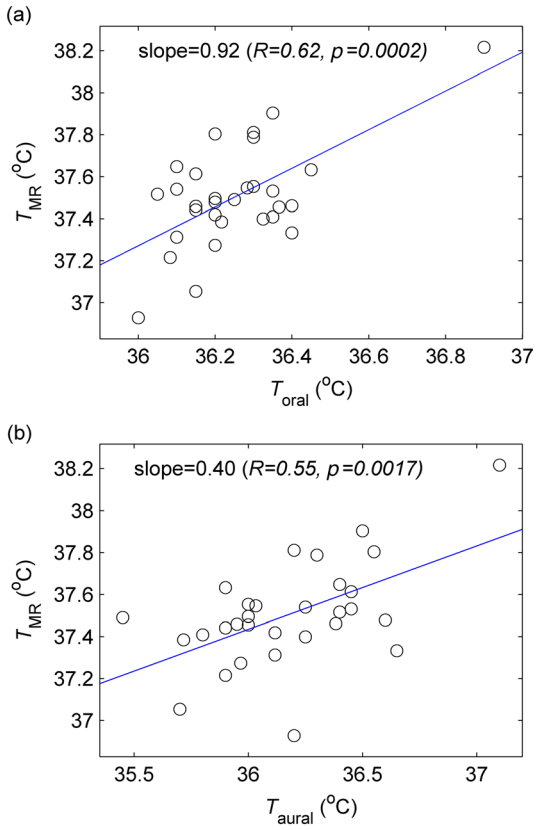

Figure 3. Brain temperature (T_{MR}) at 3 T *versus* oral (T_{oral}) (a) and aural (T_{aural}) (b) temperatures. T_{MR} represents the mean brain temperature for each subject, whereas T_{oral} and T_{aural} are the mean of pre- and post-scan measurements; measurements are averaged over all MRSI scans and visits, as described in the text.

had higher mean temperatures than those containing >25% GM (0.18/0.41 °C temperature difference at 1.5 T/3 T; $p = 0.024/<0.001$). Repetition of this analysis using only data from the 10 subjects scanned at both field strengths yielded closer values for the hemispheric temperature difference (0.18/0.19 °C at 1.5 T/3 T; $p = 0.033/0.003$), but the tissue differences were almost unchanged (0.17/0.41 °C at 1.5 T/3 T; $p = 0.046/<0.001$).

Phantom data

Good quality spectra were obtained at both field strengths (e.g. Fig. 2c, d), with 98% and 99% of voxels successfully fitted with mean NAA linewidths of 1.3 and 4.4 Hz at 1.5 and 3 T, respectively. Temperatures measured by fibre-optic thermometry were stable (SD < 0.1 °C) during all MRSI scans. To evaluate systematic drifts and errors, mean temperatures (relative to fibre-optic temperature measurements; shown in Fig. 5) in the two hemispheres were analysed using a linear mixed effects model (Table 2), with the scan session modelled as a random effect, and hemisphere and within-session scan number as fixed effects. There was a systematic difference of 0.7 °C ($p < 0.001$) between MR and fibre-optic absolute temperatures at both 1.5 and 3 T. Hemisphere dependence was not detected at 1.5 T, and was significant but very small at 3 T (0.03 °C; $p = 0.001$); thus, the temperature difference measured by MR was similar to the actual temperature difference (approximately 0.5 °C). A small mean drift in the MR–fibre-optic temperature difference was detected at 1.5 T (−0.02 °C per scan; $p = 0.041$), but not during 3-T scanning.

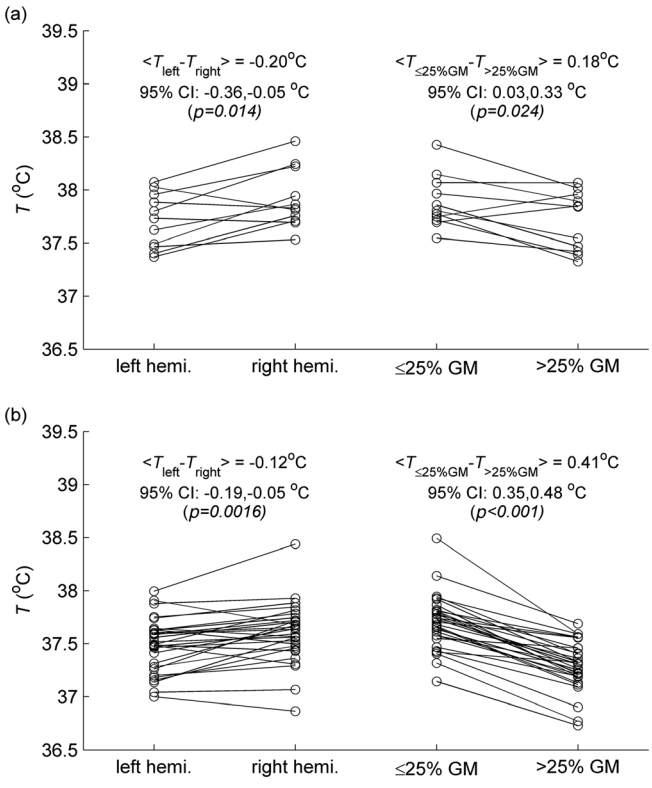

Figure 4. Within-brain temperature differences at 1.5 T (a) and 3 T (b). Paired data on the left show mean left- and right-hemisphere temperatures for each subject (mean of accepted voxels at first MRSI scan). Data on the right show the mean temperature of accepted voxels covering ≤25% grey matter (GM) and >25% GM for each subject at the first MRSI scan.

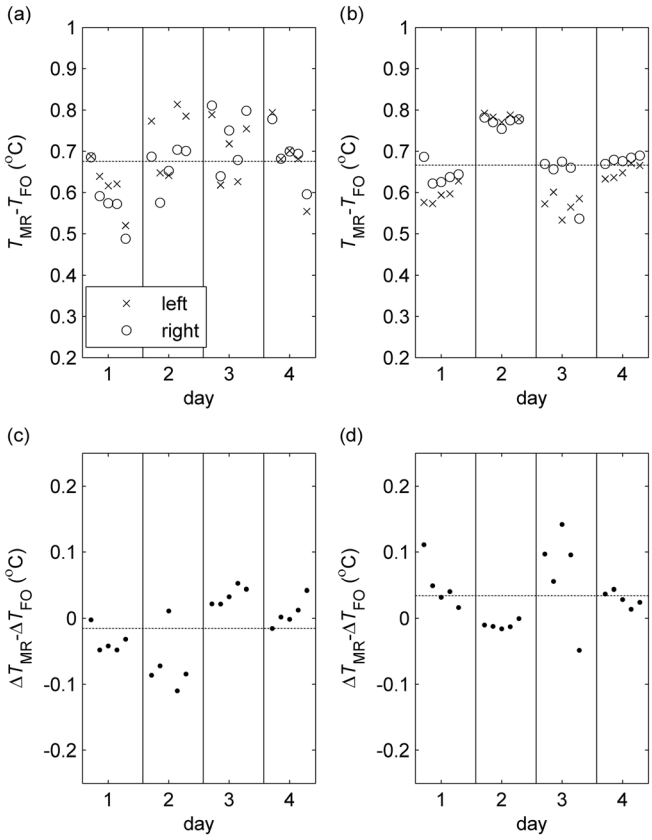

Figure 5. Error in MR temperature (T_{MR}) measured in the temperature-controlled phantom relative to temperature measured by a fibre-optic thermometer (T_{FO}) at 1.5 T (a) and 3 T (b). Mean values for the central voxels on either side of the phantom are shown for the five consecutive MRSI scans (ordered sequentially from left to right) performed on each of the four days. (c) and (d) show corresponding errors in the lateral temperature difference (right minus left) at 1.5 and 3 T, respectively. Dashed lines indicate the mean values of all data points.

DISCUSSION

The aim of this study was to investigate some of the errors that may affect MRSI temperature mapping. We found that variation between subjects was small (0.2 °C) and, as expected, independent of field strength. Inter-day variation had a similar magnitude and may reflect a combination of day-to-day changes in physiology and scanner performance; however, our study was designed to minimise diurnal effects by performing scans at a similar time of day, requiring subjects to refrain from eating and other activities that may affect brain or body temperature. The residual variability for within-session repeated measurements at 3 T (0.14 °C) was around half that measured at 1.5 T (0.36 °C), consistent with reduced errors in parameter estimation with increased sensitivity (25). Marshall *et al.* (12) reported a somewhat larger error (1.2 °C) at 1.5 T; however, the data were acquired at an inferior slice location that frequently yields poorer quality MR spectra (26), and subjects were deliberately repositioned during the scanning session. The largest component of variance at either field strength was that between different voxels (0.5–0.6 °C), consistent with the 'considerable heterogeneity' in MRSI temperature maps reported by Childs *et al.* (11).

Although the possibility of genuine within-brain temperature variation cannot be excluded [regional temperature differences have been measured invasively in conscious glioblastoma patients, for example (27)], part of this effect may be caused by differences in tissue MR properties, for example lower apparent temperatures in voxels containing significant GM. These findings reinforce recent reports by Bainbridge *et al.* (28) regarding single-voxel MRS of neonatal brain, where the apparent temperature of voxels in the thalamus was around 0.7 °C lower than that of those in WM, and by Chadzynski *et al.* (29), who scanned nine volunteers at 3 T and found a greater water–NAA chemical shift difference in voxels containing predominantly GM tissue, corresponding to a lower apparent temperature of around 1.4 °C. As discussed by these authors, the apparent temperature differences could result from systematic errors arising from a number of sources, including pH, chemical exchange of protons between water and macromolecules, and subtle susceptibility effects, some of which have been investigated recently by Vescovo *et al.* (30) and others (31). Susceptibility, for example, should have no significant effect on temperature measurements in solutions, as NAA and water protons experience the same magnetic field. However, as discussed in the articles by Chadzynski *et al.* (29) and Bainbridge *et al.* (28), *in vivo* NAA is primarily intracellular, whereas water exists in both intra- and extracellular environments; thus, tissue- and orientation-dependent variation in the magnetic susceptibilities of these compartments (32) may contribute to systematic errors in the apparent brain temperature. A single calibration, as commonly used in MRS thermometry, may therefore not be optimal for the estimation of spatial temperature variation, but appropriate tissue-specific coefficients are presently unavailable. Even if such data were determined, the large voxel sizes typically acquired in MRSI and

NMR IN BIOMEDICINE

Table 2. Linear mixed effects model analysis of phantom data. The dependent variable modelled is the mean MR temperature minus the fibre-optic temperature in each hemisphere. Scans within a session were labelled with the integer values −2 to +2 and the hemispheres were assigned values of −0.5 (left) and +0.5 (right); the intercept therefore indicates the estimated mean systematic error in the MR temperature for all scans and both hemispheres, whereas β_{hemi} represents any difference in this error between the two hemispheres (right minus left). 95% confidence intervals for parameter estimates are shown in parentheses

	Intercept (°C)	$\sigma_{session}$ (°C)	$\sigma_{residual}$ (°C)	β_{scan} (°C/scan)	$\beta_{hemisphere}$ (°C/scan)
1.5 T	0.68[c] (0.59–0.76)	0.048 (0.018–0.125)	0.068 (0.054–0.087)	−0.016[a] (−0.032 to −0.001)	−0.015 (−0.059–0.029)
3 T	0.67[c] (0.54–0.79)	0.078 (0.034–0.175)	0.030 (0.024–0.038)	−0.001 (−0.008–0.006)	0.034[b] (0.015–0.054)

[a] $p < 0.05$.
[b] $p < 0.01$.
[c] $p < 0.001$.

single-voxel MRS result in a superposition of spectra with different amplitudes, linewidths and frequencies, causing the apparent temperature to depend on multiple acquisition parameters and tissue properties. Higher resolution MRSI techniques (33) and careful voxel placement in single-voxel MRS may, in future, help to elucidate and alleviate these effects. The apparent temperature difference between the left and right hemispheres of the brain should also be interpreted cautiously, given the possibility of systematic errors. A small number of previous studies have reported lateral temperature differences in individuals (34) or in relation to behaviour during a cognitive task (35), although Ishigaki *et al.* (36) did not find a lateral temperature difference in a cohort of healthy (although older) volunteers by single-voxel MRS.

Despite these grounds for caution, there was a weak positive association between brain temperature at 3 T and independent measurements of both aural and oral temperatures; at 1.5 T, where the sample size was much smaller, there was a weak correlation between brain and aural temperatures. Bainbridge *et al.* (28) also demonstrated a positive correlation between single-voxel MRS (neonatal) brain temperature and body (rectal) temperature. We also detected small but highly significant brain cooling in both scanners during MRSI; the reduction of 0.1 °C per scan at 1.5 T was almost identical to that reported previously (12), and might be explained by a combination of subject inactivity, clothing (scrubs) with poor thermal insulation, MRSI sequences with low specific absorption rates and the intended cooling effect of scanner air flow. The mean temperatures at the four consecutive MRSI scans suggest that most of the temperature reduction occurred during the first three scans. Curiously, aural temperature increased during scanning; the oral temperature increase (detected at 3 T only) was smaller, and it is likely that part of the increase in aural temperature was caused by the wearing of ear protection during scanning (ear plugs and ear defenders were used at 3 T; ear plugs alone were used at 1.5 T, where the average aural temperature change was smaller). It should also be noted that, although MR temperature measurements specifically covered the period during MRSI acquisition, body temperature measurements were performed immediately before and after the complete MR examination, and thus reflect any temperature changes occurring during this period, e.g. during structural scans. However, the detection of subtle brain cooling effects in a small cohort supports the use of MRSI brain temperature monitoring in clinical trials, e.g. of therapeutic hypothermia.

The phantom experiments performed showed that temporal drifts and hemispheric differences were either undetectable or much smaller than those observed *in vivo*. This suggests that the apparent variation in *in vivo* temperature is not purely caused by instrumental imperfections. The systematic error of 0.7 °C between MR and fibre-optic absolute temperatures is unsurprising, given the known dependence of the water–NAA chemical shift difference on phantom composition; the discrepancy was similar at both field strengths, consistent with a recent calibration study at 3 T (31).

A limitation of the present study is that MRSI scanning was performed on one slice and with limited resolution; although this limited our ability to distinguish between different tissues, the acquisition parameters used are representative of those in use or available at most institutions. Although we attempted to acquire 1.5- and 3-T data using similar protocols, differences in the hardware and software could potentially have influenced our findings. As discussed above, the calibration coefficients used in any study of *in vivo* human brain temperature by MRS are somewhat arbitrary because of the lack of a non-invasive gold standard technique. Nevertheless, although temperatures derived from published calibrations [see table 1 of ref. (30)] may differ systematically by up to several degrees Celsius, most groups have found the relationship between temperature and $\Delta\delta$ to be highly linear, with good agreement regarding the slope. The calibration should therefore have little influence on our measurements of variability and cooling. The data quality was typically good, with approximately 15% of voxels rejected on quality grounds (after voxel content criteria had been applied). There was a tendency for voxels in which NAA fitting was rejected to be located at the anterior part of the region of interest, where magnetic field homogeneity is typically poorer, and at the edges of the brain, where spectra may be contaminated by unsuppressed lipid. Rejection as a result of poor NAA fitting was more frequent at 1.5 T than at 3 T, which is unsurprising given the lower signal-to-noise ratio achievable at 1.5 T. Rejection as a result of water resonance distortion was more common at 3 T. As this occurred frequently in the vicinity of the lateral ventricles (the example shown in Fig. 1b is typical), residual CSF contamination may be implicated.

CONCLUSIONS

We have quantified sources of variability associated with MRSI brain temperature mapping and have shown the precision of repeated measurements to be somewhat higher at 3 T than at 1.5 T. Brain temperature was positively associated with independent measures of head temperature, and we were able to detect very small changes in brain temperature during MRSI scanning. We hope that such data will enable future clinical studies to be efficiently designed and sufficiently powered.

Acknowledgements

We wish to acknowledge the following for support of this study: funding from the Chief Scientist Office of Scotland (grant ETM/3); 1.5-T imaging (E10836) was carried out at the Brain Research Imaging Centre and 3-T imaging was performed at the Clinical Research Imaging Centre; the centres are part of the University of Edinburgh Wellcome Trust Clinical Research Facility and the SINAPSE (Scottish Imaging Network: A Platform for Scientific Excellence) collaboration, funded by the Scottish Funding Council and the Chief Scientist Office of Scotland; the Clinical Research Imaging Centre is also supported by the British Heart Foundation; radiology and radiography staff at the University of Edinburgh; Dr Craig Buckley and Dr Christian Schuster (Siemens) for assistance with 3-T MRSI; JP acknowledges financial support from SINAPSE and a University of Edinburgh Overseas Research Studentship award; BAH and SIKS acknowledge the financial support of NHS Research Scotland, through NHS Lothian.

REFERENCES

1. Greer DM, Funk SE, Reaven NL, Ouzounelli M, Uman GC. Impact of fever on outcome in patients with stroke and neurologic injury: a comprehensive meta-analysis. Stroke 2008; 39(11): 3029–3035.
2. Dippel DWJ, van Breda EJ, van der Worp HB, van Gemert HMA, Kappelle LJ, Algra A, Koudstaal PJ. Timing of the effect of acetaminophen on body temperature in patients with acute ischemic stroke. Neurology 2003; 61(5): 677–679.
3. Mariak Z. Intracranial temperature recordings in human subjects. The contribution of the neurosurgeon to thermal physiology. J. Thermal Biol. 2002; 27(3): 219–228.
4. Harris B, Andrews P, Murray G, Forbes J, Moseley O. Systematic review of head cooling in adults after traumatic brain injury and stroke. Brain Inj. 2012; 26(4–5): 372–372.
5. Mrozek S, Vardon F, Geeraerts T. Brain temperature: physiology and pathophysiology after brain injury. Anesthesiol. Res. Pract. 2012; 2012: 989487.
6. Rieke V, Pauly KB. MR thermometry. J. Magn. Reson. Imaging 2008; 27(2): 376–390.
7. McDannold N Quantitative MRI-based temperature mapping based on the proton resonant frequency shift: review of validation studies. Int. J. Hyperthermia, 2005; 21(6): 533–546.
8. Corbett RJT, Laptook AR. Failure of localized head cooling to reduce brain temperature in adult humans. NeuroReport 1998; 9(12): 2721–2725.
9. Harris BA, Andrews PJD, Marshall I, Robinson TM, Murray GD. Forced convective head cooling device reduces human cross-sectional brain temperature measured by magnetic resonance: a non-randomized healthy volunteer pilot study. Br. J. Anaesthesia 2008; 100(3): 365–372.
10. Cady EB, D'Souza PC, Penrice J, Lorek A. The estimation of local brain temperature by in-vivo H-1 magnetic-resonance spectroscopy. Magn. Reson. Med. 1995; 33(6): 862–867.
11. Childs C, Hiltunen Y, Vidyasagar R, Kauppinen RA. Determination of regional brain temperature using proton magnetic resonance spectroscopy to assess brain–body temperature differences in healthy human subjects. Magn. Reson. Med. 2007; 57(1): 59–66.
12. Marshall I, Karaszewski B, Wardlaw JM, Cvoro V, Wartolowska K, Armitage PA, Carpenter T, Bastin ME, Farrall A, Haga K. Measurement of regional brain temperature using proton spectroscopic imaging: validation and application to acute ischemic stroke. Magn. Reson. Imaging 2006; 24(6): 699–706.
13. Karaszewski B, Wardlaw JM, Marshall I, Cvoro V, Wartolowska K, Haga K, Armitage PA, Bastin ME, Dennis MS. Measurement of brain temperature with magnetic resonance spectroscopy in acute ischemic stroke. Ann. Neurol. 2006; 60(4): 438–446.
14. Karaszewski B, Wardlaw JM, Marshall I, Cvoro V, Wartolowska K, Haga K, Armitage PA, Bastin ME, Dennis MS. Early brain temperature elevation and anaerobic metabolism in human acute ischaemic stroke. Brain 2009; 132: 955–964.
15. Whiteley WN, Thomas R, Lowe G, Rumley A, Karaszewski B, Armitage P, Marshall I, Lymer K, Dennis M, Wardlaw J. Do acute phase markers explain body temperature and brain temperature after ischemic stroke? Neurology 2012; 79(2): 152–158.
16. Scheenen TWJ, Klomp DWJ, Wijnen JP, Heerschap A. Short echo time H-1-MRSI of the human brain at 3T with minimal chemical shift displacement errors using adiabatic refocusing pulses. Magn. Reson. Med. 2008; 59(1): 1–6.
17. Brown MA. Time-domain combination of MR spectroscopy data acquired using phased-array coils. Magn. Reson. Med. 2004; 52(5): 1207–1213.
18. Serrai H, Clayton DB, Senhadji L, Zuo C, Lenkinski RE. Localized proton spectroscopy without water suppression: removal of gradient induced frequency modulations by modulus signal selection. J. Magn. Reson. 2002; 154(1): 53–59.
19. Vanhamme L, van den Boogaart A, Van Huffel S. Improved method for accurate and efficient quantification of MRS data with use of prior knowledge. J. Magn. Reson. 1997; 129(1): 35–43.
20. Pijnappel WWF, Vandenboogaart A, Debeer R, Vanormondt D. Svd-based quantification of magnetic-resonance signals. J. Magn. Reson. 1992; 97(1): 122–134.
21. Naressi A, Couturier C, Devos JM, Janssen M, Mangeat C, de Beer R, Graveron-Demilly D. Java-based graphical user interface for the MRUI quantitation package. Magn. Reson. Mater. Phys. Biol. Med. 2001; 12(2–3): 141–152.
22. Jenkinson M, Bannister P, Brady M, Smith S. Improved optimization for the robust and accurate linear registration and motion correction of brain images. Neuroimage 2002; 17(2): 825–841.
23. Smith SM. Fast robust automated brain extraction. Hum. Brain Mapping 2002; 17(3): 143–155.
24. Zhang YY, Brady M, Smith S. Segmentation of brain MR images through a hidden Markov random field model and the expectation-maximization algorithm. IEEE Trans. Med. Imaging 2001; 20(1): 45–57.
25. Cavassila S, Deval S, Huegen C, van Ormondt D, Graveron-Demilly D. Cramer–Rao bound expressions for parametric estimation of overlapping peaks: influence of prior knowledge. J. Magn. Reson. 2000; 143(2): 311–320.
26. Parikh J. Measurement of brain temperature using magnetic resonance spectroscopic imaging. PhD Thesis, University of Edinburgh, 2012.
27. Whittle IR, Stavrinos N, Akil H, Yau Y, Lewis SC. Assessment of physiological parameters within glioblastomas in awake patients: a prospective clinical study. Br. J. Neurosurg. 2010; 24(4): 447–453.
28. Bainbridge A, Kendall GS, Vita ED, Hagmann C, Kapetanakis A, Cady EB, Robertson NJ. Regional neonatal brain absolute thermometry by (1) H MRS. NMR Biomed. 2013; 26(4): 416–423.
29. Chadzynski GL, Bender B, Groeger A, Erb M, Klose U. Tissue specific resonance frequencies of water and metabolites within the human brain. J. Magn. Reson. 2011; 212(1): 55–63.
30. Vescovo E, Levick A, Childs C, Machin G, Zhao S, Williams SR. High-precision calibration of MRS thermometry using validated temperature standards: effects of ionic strength and protein content on the calibration. NMR Biomed. 2013; 26(2): 213–223.
31. Babourina-Brooks B, Simpson R, Arvanitis TN, Peet AC, Davies NP. An accurate calibration of MRS thermometry at 3 T. *Proceedings of the 21st Annual Meeting ISMRM*, Salt Lake City, UT, USA, 2013; 533.
32. He X, Yablonskiy DA. Biophysical mechanisms of phase contrast in gradient echo MRI. Proc. Natl. Acad. Sci. U. S. A. 2009; 106(32): 13 558–13 563.
33. Ebel A, Maudsley AA. Improved spectral quality for 3D MR spectroscopic imaging using a high spatial resolution acquisition strategy. Magn. Reson. Imaging 2003; 21(2): 113–120.
34. Landolt HP, Moser S, Wieser HG, Borbely AA, Dijk DJ. Intracranial temperature across 24-hour sleep–wake cycles in humans. NeuroReport 1995; 6(6): 913–917.
35. Helton WS. The relationship between lateral differences in tympanic membrane temperature and behavioral impulsivity. Brain Cognition 2010; 74(2): 75–78.
36. Ishigaki D, Ogasawara K, Yoshioka Y, Chida K, Sasaki M, Fujiwara S, Aso K, Kobayashi M, Yoshida K, Terasaki K, Inoue T, Ogawa A. Brain temperature measured using proton MR spectroscopy detects cerebral hemodynamic impairment in patients with unilateral chronic major cerebral artery steno-occlusive disease; comparison with positron emission tomography. Stroke 2009; 40(9): 3012–3016.

